JMEPEG (2010) 19:611–615
DOI: 10.1007/s11665-009-9530-7

1059-9495/$19.00

Numerical Analysis of Residual Stress for Copper Base Brazed Stainless Steel Plate-Fin Structure

Qiaoyun Xie and Xiang Ling

(Submitted January 12, 2009; in revised form July 10, 2009)

Copper base stainless steel plate-fin structure has been widely used as a heat exchanger in many fields. The nonlinear thermal reaction on the residual stress in brazing process of the plate-fin structure was studied in this paper. A finite element model (FEM) was proposed to simulate the heat transfer and the sequential residual stress generated in the plate-fin and filler metals based on thermal elastic-plastic theory. By the stress distribution in four paths marked in the structure obtained from FEM results, it is found that the maximum residual tensile stress occurs in the brazed joint next to the plate side and a crack would initiate in this region. Also, the first principle stresses of reference nodes were calculated and the conclusion is consistent with the simulation results. These results would provide some constructive instructions in the practical brazing procedure.

Keywords brazed residual stress, FEM, first principle stress, thermal elastic-plastic

1. Introduction

Plate-fin heat exchangers, as a type of compact exchangers, are becoming important components in the fields of electronics, aerospace, and petrochemical engineering (Ref 1). Basically, a PEHE is comprised of layers of corrugated fins separated from one another by flat plates, typically stainless steels, and seals along the edges with bars (Ref 2, 3). Prior studies have shown that the vacuum brazing has been proved to be a good method to manufacture stainless steel PEHE due to its significant reduction in size, weight, and footprint to save, and also very large area per unit volume combined with very high heat transfer coefficients (Ref 4, 5). The fins and the plates are connected during fusion of the filler metals in between by elevating the temperature to an optimum value. Copper and copper-based alloys are representative filler metals in brazing technologies distinguished by excellent wetting and flowing abilities (Ref 6). More recent papers have described experiments and research relating to the problems encountered in the process of brazing, among which the most serious problem is the large residual stress (Ref 7-9). As a result of the joint influence of self-restraint, fixture, thermal cycling and small thickness of fins and plates, it is of significant importance to control the residual stress and thermal deformation during the integral forming of plate-fin structure in the furnace brazing in order to obtain a desirable manufacturing accuracy and reliability (Ref 10-12). Inevitable residual stresses developed in the braze process due to large differences in the thermal expansion coefficients will increase the susceptibility to brittle fracture, fatigue damage, and stress corrosion cracking (Ref 13). In addition, the presence of residual stress would have a great impact on the creep deformation, which is the major failure mode, when the structure is served in high temperature conditions (Ref 14).

In this work, the software of ABAQUS was adopted to simulate the brazing temperature field for the joint between SS304 plate-fins to pure copper fillers and the sequential coupling thermal residual stress.

2. Calculation Steps

2.1 Assumptions

In view of the complexity of practical brazing procedure, such as the metallurgical reaction, the diffusion reaction, and the microstructure change of joint, some issues would be assumed and simplified in the simulation: (1) Both the base metal SS304 and the copper filler are supposed to take an elastic-plastic deformation. (2) Both the materials are treated as isotropic, linear elastic and plastic, and the mechanical and physical property parameters are assumed to be temperature dependent. (3) The dissolution and diffusion of filler metal to base metal, and the flow of liquid filler metal at brazing temperature are ignored. (4) The capillary reaction of filler metal is also ignored.

2.2 Calculation of Residual Stress

For the thermal elastic-plastic FEM calculation of the residual stress for copper base brazed stainless steel plate-fin structure unit in this paper, stresses in the following directions were defined for evaluating the brazed structure: σ_{11} in one-direction, σ_{22} in two-direction, τ_{12} in 12-plane. Based on the principle distortion energy theory, cracking and extension of

Qiaoyun Xie and **Xiang Ling**, School of Mechanic and Power Engineering, Nanjing University of Tech, 210009 Nanjing, P.R. China. Contact e-mail: xling@njut.edu.cn.

planar fracture can be investigated by first and second principle stresses (Ref 15):

$$\begin{Bmatrix} \sigma_1 \\ \sigma_2 \end{Bmatrix} = \frac{(\sigma_{11} + \sigma_{22})}{2} \pm \frac{1}{2}\sqrt{(\sigma_{11} - \sigma_{22})^2 + 4\tau_{12}^2} \qquad \text{(Eq 1)}$$

where σ_1 is first principle stress; σ_2, second principle stress; σ_{11}, longitudinal stress; σ_{22}, transverse stress; and τ_{12}, shear stress.

According to this evaluation standard for joint cracking, the initial cracking location of brazed joint is corresponding with the maximum value of first principle stress and the extension of the crack matches with the distribution of second principle stress. Only the first principle stress is of concern in the paper, aiming at verifying the conclusion drawn by simulation.

3. FEM-Techniques Using ABAQUS

3.1 Simulation Parameters

Due to periodical repetition of the plate-fin structure, only a unit of the plate-fin was studied. Figure 1 depicts the geometrical size of the unit in detail. Table 1 lists material properties for pure copper and SS304, which were obtained by thermal analysis experiments and tensile test at high temperature.

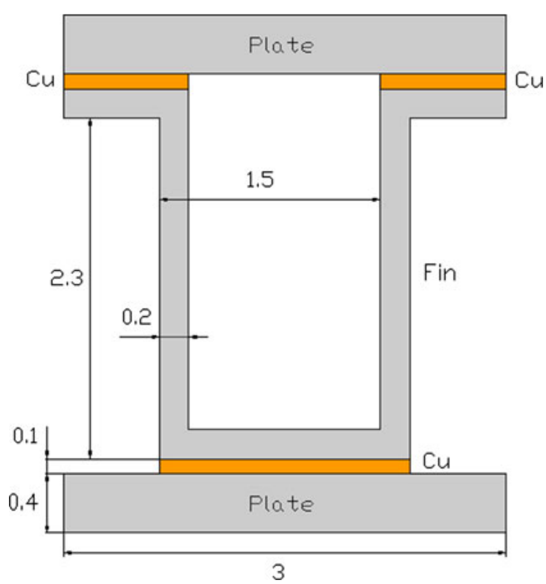

Fig. 1 Sketch diagram of the plate-fin structure

The reduced integration of C2D4R continuum element and CPE4R plane strain element, with four integration points of Standard FE was used in the transient heat transfer and stress analysis, respectively. Figure 2 shows the FE meshed model of the plate-fin unit, with 2188 nodes and 1984 elements.

3.2 Boundary Conditions

Figure 3 shows the seven temperature stages in the vacuum brazing: (1) vacuum pumping; (2) heating to 950 °C (5700 s); (3) holding at 950 °C (1800 s); (4) heating to the brazing temperature 1140 °C (2280 s); (5) holding at 1140 °C (3600 s); (6) furnace cooling (2400 s); and (7) natural cooling (4200 s). The temperature curve should be applied in the thermal analysis for all the nodes. Besides, transient heat transfer generated by furnace radiation as well as the heat lost in this procedure need to be considered. Regards to the cavity enclosed by fins and plates where furnace radiation cannot work, cavity radiation ought to be added (Ref 16, 17). The reaction of heat reflection is expressed as (Ref 18):

$$q_i = Bw_i \sum_j w_j \sum_k F_{ik} C_{kj}^{-1} \left(T_j^4 - T_i^4 \right) \qquad \text{(Eq 2)}$$

where q is unit heat flux; B, Stefan-Boltzmann constant; w, surface emissivity; F, view factor; C reflection matrix of surface; and T, temperature.

As for the stress analysis, the temperature obtained in the former step was loaded in all the nods as the temperature field boundary. Further, nodes on the lower surface were constrained in two-direction, and those on the leftmost and rightmost surfaces were constrained in one-direction. Besides, a uniformed load of 0.5MP was distributed on the top surface to simulate the loads generated by the claming fixture, as depicted in Fig. 2.

4. Results and Discussion

In the residual distribution field, there was a distinct stress gradient in the brazed joint. For the sake of a better understanding, four reference paths were selected, as marked in Fig. 2. Path P1 is the interface between the fin and filler; path P2 is in the middle of the brazed joint; path P3 is the interface between the filler and the plate; path P4 is passing though the fin, the fillet, and the plate all together.

Table 1 Material parameters used in FEM simulation

Material	Temperature, °C	Conductivity, W m/°C	Specific heat, J/(kg °C)	CET (10^{-6}), 1/°C	E, GPa	Poisson's ratio	Yield stress, MPa
SS304	20	15.26	504	16.0	199	0.28	206
	400	20.2	582	18.1	166	0.26	108
	600	22.8	634	18.6	150	0.25	82
	1000	28	738	20.0	100	0.24	48
Pure copper	20	400.68	383.48	16.8	117	0.34	210.74
	400	422.42	374.65	18.3	92	0.32	110
	600	360.96	473.82	23.1	84	0.31	10
	1000	331.68	504.00	39.7	30	0.31	...

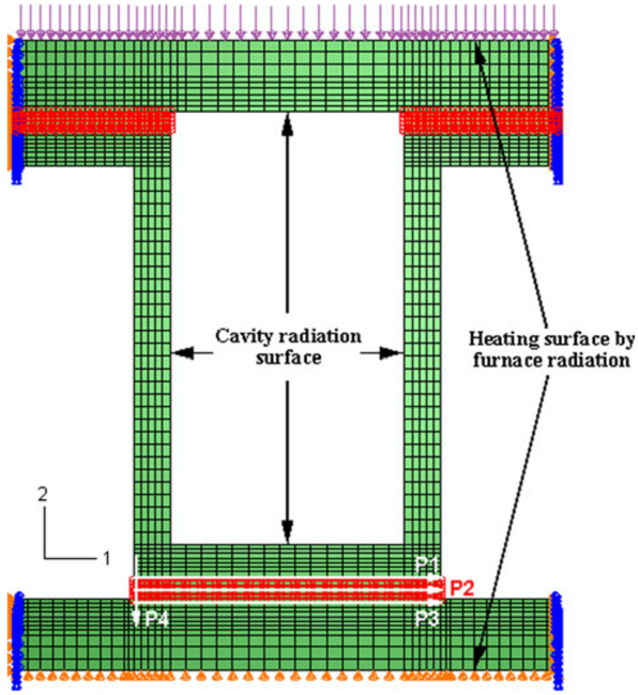

Fig. 2 FE model

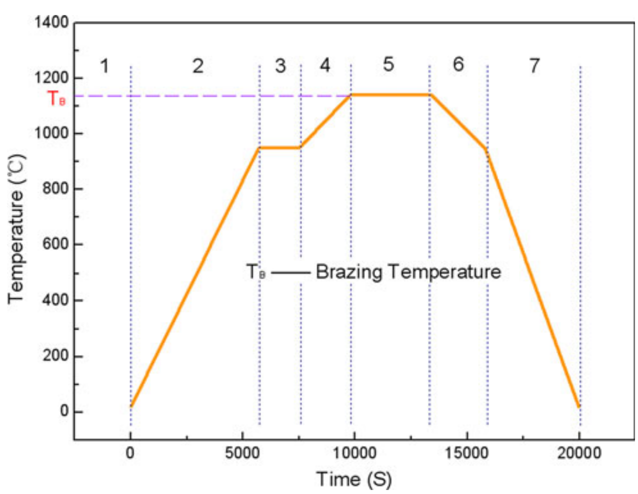

Fig. 3 Steps for whole brazing process

Figures 4-6 exhibit the residual stress distribution of the three paths in the bottom filler, respectively. From the three figures, the two normal stresses are symmetrically distributed while the shear stress is unsymmetrical. It also can be seen that the longitudinal stresses are prominent while the transverse and shear stresses are relatively small. It is the longitudinal stress that has the main influence on the strength of the filler metal.

In Fig. 4, transverse and shear stress have their peak values (28.9 MPa for σ_{22} and 59.2 MPa for τ_{12}) on the two ends of the path while the maximal longitudinal stress (140.3 MPa) locates on the middle of the path. The same conclusion could be drawn for path 2 in Fig. 5. But its peak stress values (142.5 MPa for σ_{11}, 52.4 MPa for σ_{22}, and 81.1 MPa for τ_{12}) are larger than those of path 1.

In Fig. 6, it can be easily found that the longitudinal stress has transferred its peak value location from the middle part to

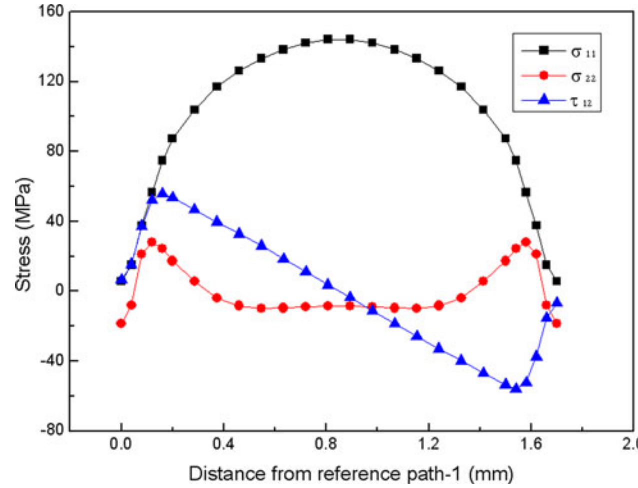

Fig. 4 Residual stress distribution of P1

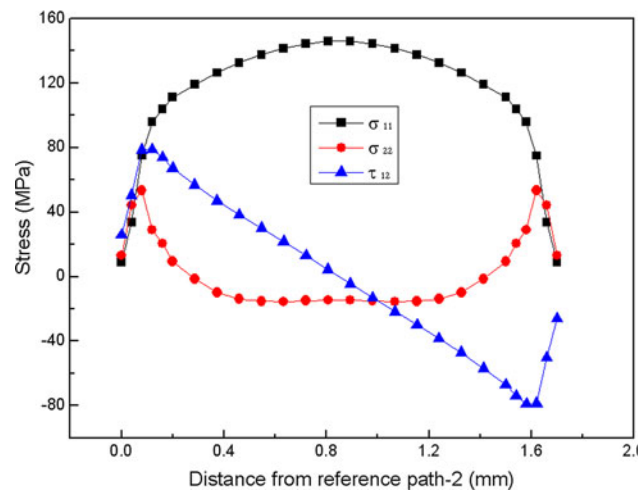

Fig. 5 Residual stress distribution of P2

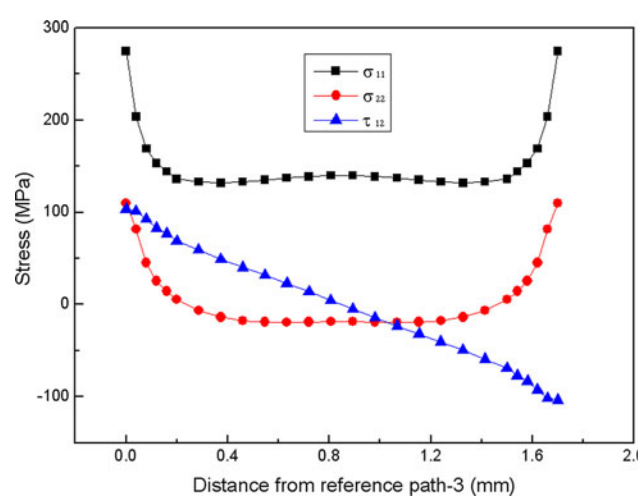

Fig. 6 Residual stress distribution of P3

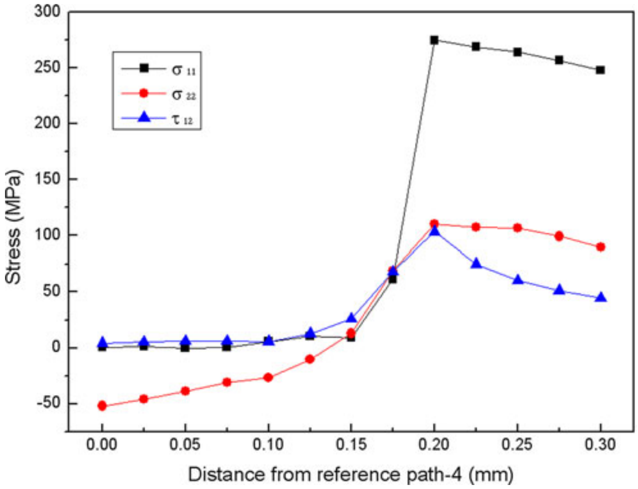

Fig. 7 Residual stress distribution of P4

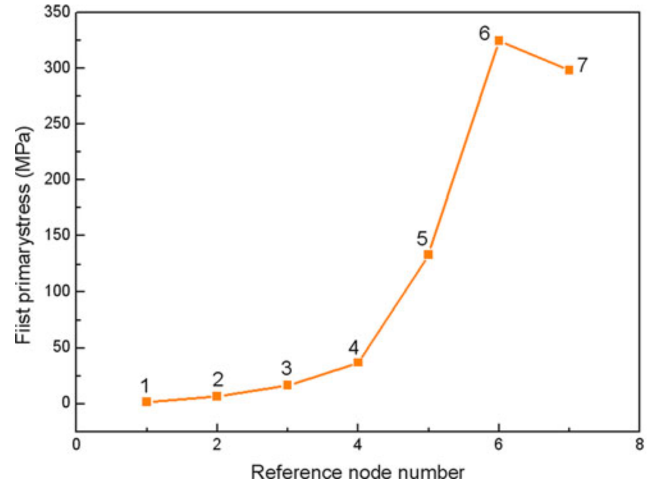

Fig. 9 First principle stress for reference nodes

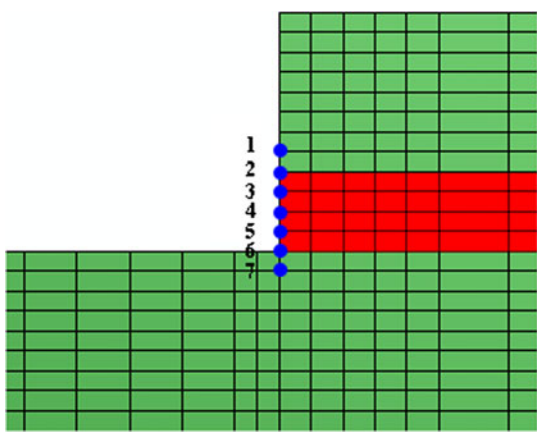

Fig. 8 Reference nodes in path P4

the ends of the path. Actually, all the three stress components have their maximum values on the two terminals of the path. This is because the melting filler copper is squeezed out of the brazing seam, forming small transitional arcs in the two ends, which are known for brazed joints. Due to the mismatching thermal expansion coefficients between copper filler metal and SS304 base metal in the heating stage as well as the dissimilar shrinkage in the cooling process, the largest residual stress occurs in the region of brazed joint. The maximum longitudinal stress is as large as 274.8 MPa, which has exceeded the yield stress of copper. When the plate-fin structure is served under extreme conditions (high temperature, high pressure, and corrosion), the high tensile residual stress in the brazed joint would induce stress cracking and result in failure, eventually.

Figure 7 displays the residual stress distribution of path P4. The stress gradient around the brazed joint is much large. In the vertical direction, the transverse and shear stresses of fin are around zero. When approaching the brazed joint, the residual stress is presented with a remarkable elevating trend and reaches the highest value in the interface between base metal and filler. While in the plate, the values of stress decrease a little, but are much higher than those in the fin. The same conclusion can be drawn that the brazed joint near the plate side suffers the maximum residual stress.

Figure 8 shows reference nodes selected in path P4, and Fig. 9 presents the first principle stress for each node. From the calculated results, it is visible that points 6 and 7 which located in the brazed joint near the top surface of the plate are with higher values. This means that the cracking failure would occur in the area of brazed joint next to the plate side firstly.

5. Conclusions

In this work, the residual stress in copper base brazing stainless steel PFHE was presented by means of heat transfer and a sequential thermal-mechanical coupling standard FEM codes in ABAQUS.

The brazing temperature field obtained in the transient thermal analysis was successfully added into the stress analysis based on thermal elastic-plastic theory in order to get the brazing residual stress. The brazed joints of plate-fin structure suffer the largest residual stress due to expansion and shrinkage caused by the material properties mismatch between copper filler metal and SS304 base metal, which makes the joint highly susceptible to cracking. The conclusion is also verified by studying of first principle stress, which is used to estimate crack extension of planar fracture basing on the principle distortion energy theory.

Acknowledgments

The authors acknowledge the financial support provided by funds of the program for new century excellent talents in university (Grant No. NCET-07-0434) and Jiangsu Key Technology R&D Program (Grant No. BE 2008005).

References

1. Z. Zhang and Y. Li, CFD Simulation of on Inlet Configuration of Plate-Fin Heat Exchangers, *Cryogenics*, 2006, **43**(12), p 673–678
2. Alpema, The Standards of the Brazed Aluminum Plate-Fin Heat Exchanger Manufacturer's Association (Alpema), 2nd ed., 2000
3. H. Peng and X. Ling, Optimal Design Approach for the Plate-Fin Heat Exchangers Using Neural Networks Cooperated with Genetic Algorithms, *Appl. Therm. Eng.*, 2008, **28**(5-6), p 642–650

4. W. Diery, Manufacture of Plate-Fin Heat Exchangers at Linde, *Linder Rep. Sci. Tech.*, 1984, **37**, p 187–203
5. T. Alberto and F. Massardo Aristide, Optimal Design of Compact Recuperation for Microturbine Application, *Appl. Therm. Eng.*, 2005, **25**, p 2054–2071
6. Y.L. Shabtay et al., New Brazing Processes Using Anneal-Resistant Copper and Brass Alloys, *Mater. Des.*, 2003, **25**(2004), p 83–89
7. V. Cazajus et al., Thermo-Mechanical Behaviour of Ceramic Metal Brazed Assemblies, *J. Mater.*, 2008, **222**(4), p 291–297
8. Kar. Abhijit et al., Effect of Interfacial Thickness and Residual Stress on the Mechanical Property of the Alumina-Stainless Steel Brazed Joint Interface, *J. Mater. Sci. Eng.*, 2008, **498**(1–2), p 283–288
9. S.-M. Chen and S.-T. Lin, Brazing Diamond Grits onto a Steel Substrate Using Copper Alloys as the Filler Metals, *J. Mater. Eng. Perform.*, 1996, **5**(6), p 761–766
10. E. Chang and C.-H. Chen, Low-Melting-Point Titanium-Base Brazing Alloys—Part 2: Characteristics of Brazing Ti-21Ni-14Cu on Ti-6Al-4V Substrate, *J. Mater. Eng. Perform.*, 1997, **6**(6), p 797–803
11. Y. Arai, M. Kikuchi, and T. Watanabe, Residual Stress Due to Welding and Its Effect on the Assessment of Cracks Near the Weld Interface, *Int. J. PVP*, 1995, **3**, p 237–248
12. L. Qianchu, Modeling the Effect of Welding Residual Stresses on Fracture Toughness of a Welded Joint, *Int. J. PVP*, 1997, **2**, p 103–109
13. D. Aquaro and M. Pieve, High Temperature Compact Heat Exchangers: Performance of Advanced Metallic Recuperators for Power Plants, *Proceedings of Fifth International Conference on Enhanced, Compact and Ultra-Compact Heat Exchangers: Science, Engineering and Technology*, Hoboken, NJ, USA, 2005, p 239–246
14. J.J. Stephens, S.N. Burchett, and F.M. Hosking, Residual Stresses in Metal-Ceramic Brazes: Effect of Creep on Finite Element Analysis Results, *Metal Ceram. Join.*, 1991, **23–41**, p 15
15. J. Yuzhe and J.J. Stephens, Residual Stress in Metal to Ceramic Brazing Joints, *International Brazing & Soldering Conference Proceedings*, Aluquerque, New Mexico, 2000, p 411–418
16. Y.J. Chao et al., Heat Transfer in Friction Stir Welding-Experimental and Numerical Studies, *J. Manuf. Sci. Eng.*, 2003, **125**(1), p 138–145
17. D. Yao and P. Nagarajan, A Strategy for Rapid Thermal Cycling of Models in Thermaloplastic Processing, *J. Manuf. Sci. Eng.*, 2006, **128**(4), p 837–843
18. Hibbitt, Karisson & Sorensen, Inc, *Heat Transfer Thermal-Stress Analysis with ABAQUS*, Providence, RI, 2000